



Evaluation of 2,6-difluoro-3-(oxazol-2-ylmethoxy)benzamide chemotypes as Gram-negative FtsZ inhibitors

Jesus D. Rosado-Lugo¹ · Yangsheng Sun¹ · Anamika Banerjee¹ · Yanlu Cao¹ · Pratik Datta¹ · Yongzheng Zhang¹ · Yi Yuan¹ · Ajit K. Parhi¹

Received: 7 February 2022 / Revised: 18 April 2022 / Accepted: 21 April 2022
© The Author(s), under exclusive licence to the Japan Antibiotics Research Association 2022

Abstract

FtsZ inhibitors represent a new drug class as no drugs using this mode of action (MOA) have been approved by regulators. 3-alkoxy substituted 2,6-difluorobenzamide scaffold is one of the most studied FtsZ inhibitors among which the most promising anti-MRSA candidate TXA709 is in clinical trial. In this paper, we present the screening and evaluation of a benzamide class that is functionalized at the alkoxy fragment targeting Gram-negative bacteria. The variations in 3-alkoxy substitutions, specifically the hydroxylated alkyl residues to the secondary and stereogenic pseudo-benzylic carbon of their methyleneoxy linker, are particularly active against *K. pneumoniae* ATCC 10031 in marked contrast to the derivatives related to PC190723, all of which were inactive against Gram-negative bacteria. The two lead molecules TXA6101 and TXY6129 inhibit the polymerization of *E. coli* FtsZ in a concentration-dependent manner and induce changes in the morphology of *E. coli* and *K. pneumoniae* consistent with inhibition of cell division. These classes of compounds, however, were found to be substrates for efflux pumps in Gram-negative bacteria.

Introduction

In 2018, WHO's new Global Antimicrobial Surveillance System (GLASS) revealed widespread incidence of antibiotic resistance among 500,000 people with suspected bacterial infections across 22 nations, including developing and developed parts of the world [1–4]. This report recognized three out of five of the most commonly prevalent antibiotic-resistant bacteria responsible for the global epidemic as *Escherichia coli*, *Klebsiella pneumoniae* and *Salmonella* spp., all belonging to the Enterobacteriaceae family. Both *Klebsiella* and *E. coli* also appear on lists of germs that are difficult to treat because they have high levels of resistance to antibiotics, including carbapenems [5, 6].

FtsZ is an essential protein for bacterial cell division and viability [7, 8]. During bacterial binary division, FtsZ self-polymerizes in a GTP-dependent manner to form a highly dynamic structure, called the “Z” ring, at the bacterial

mid-cell. This structure becomes anchored to the bacterial membrane and acts as a scaffold for the recruitment of other cellular proteins to assemble the septum and guide the cell division process. FtsZ is highly conserved and ubiquitous across most bacterial groups. Inactivation of FtsZ causes the bacteria to develop an elongated filamentous morphology due to the inability of daughter cells to separate from one another, and the bacteria ultimately lyse (Fig. 1) [9].

FtsZ has been considered an excellent target for antimicrobial drug discovery for several key reasons, as it is: an essential protein for bacterial viability; highly conserved and has been identified in most bacteria; potentially a broad-spectrum antibacterial target; not present in eukaryotic cells, potentially minimizing off-target effects and consequent toxicity in humans and; a novel target, as there are no FtsZ-targeting antimicrobial drugs on the market and no cross-resistance with other classes of drugs has been observed [10–16].

The appeal of FtsZ as an antibacterial target led to the discovery of PC190723 at Prolysis, Ltd. [17]. One of the principal limitations that restricted the clinical utility of this compound is its poor solubility. The hydrophobic nature of the compound made it difficult to formulate in a vehicle suitable for in vivo therapy. TAXIS Pharmaceuticals Inc elucidated that the chloride atom of PC190723 is the

✉ Ajit K. Parhi
aparhi@taxispharma.com

¹ TAXIS Pharmaceuticals, Inc., R&D Department, 9 Deer Park Drive, Suite J-15, Monmouth Junction, NJ 08852, USA

Fig. 1 The functional inhibition of FtsZ blocks cell division

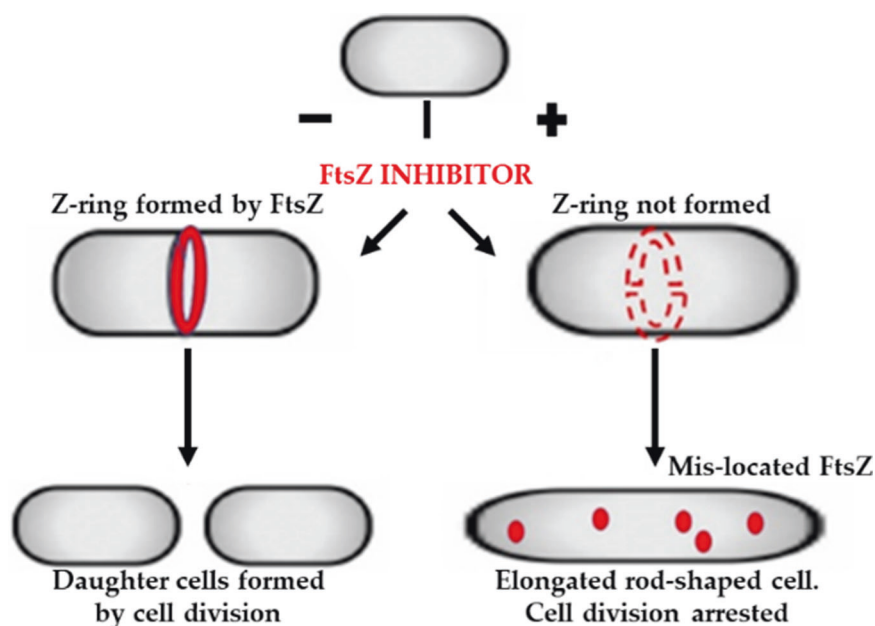


Fig. 2 Structures of PC190723, TXA707, and TXA709

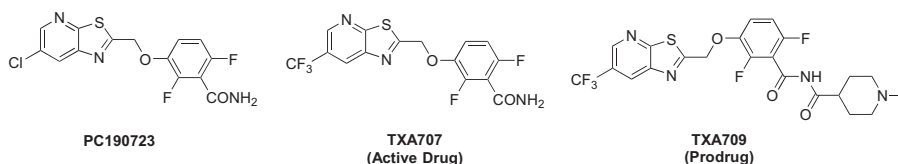
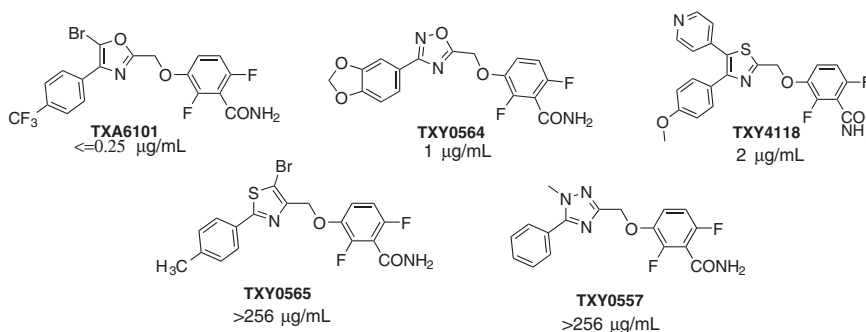


Fig. 3 Structures of novel five-membered heterocyclic substituted benzamides with intrinsic MIC against MSSA ATCC 19636



primary site susceptible to metabolic attack, leading to rapid elimination by de-chlorination and mono-oxygenation [18–20]. Substitution of the chloride atom with a trifluoromethyl group yielded TXA707 and its prodrug, TXA709 [20, 21], that overcame the undesired properties of PC190723 (Fig. 2), thus becoming the first FtsZ-targeting antibiotic to enter human clinical trials.

During the development of Gram-positive FtsZ inhibitors we have also explored other heterocycles (both fused and non-fused) from six- and five-membered ring families, each retaining the difluoro-benzamide structure [22, 23]. Some of the five-membered heterocycles explored in our anti-MRSA program are shown in Fig. 3. These novel, heterocyclic benzamide chemotypes have varying degrees of FtsZ affinities and intrinsic potency against MRSA and MSSA.

Particularly the benzamide derivative that belongs to the oxazole chemotype TXA6101 (Fig. 3) is especially noteworthy, having a minimum inhibitory concentration (MIC) of $0.25 \mu\text{g mL}^{-1}$ against MRSA and MSSA.

Recently we have reported that structural flexibility of FtsZ inhibitors like TXA6101 relative to TXA707 is a key factor for overcoming drug-resistant mutations in the protein and offer a structural basis for the design of new FtsZ inhibitors with high potency and extended antibacterial coverage (Fig. 4) [24]. In this work, we are reporting the results of our investigations on the TXA6101 chemotype as inhibitors of Gram-negative FtsZ and potential new treatment against Gram-negative infections. During the anti-MRSA program we realized that the TXA6101 chemotypes from the oxazole-benzamide class are particularly appealing

over other small molecule FtsZ inhibitors for their enhanced metabolic stability, solubility, and favorable pharmacokinetic profiles. The favorable drug-like properties of these small molecules thus make this series more likely to succeed than any of the others against Gram-negative pathogens.

Results and discussion

Sequence alignment of FtsZ from multiple bacteria

To investigate how effective these classes of inhibitors could be for Gram-negative bacterial FtsZ, we aligned the amino acid sequences comprising enzymatic regions of the protein available from the UniProt database for *E. coli*, *K. pneumoniae*, *Shigella sonnei*, *Proteus mirabilis* and compared them with other Gram-negative and Gram-positive pathogens, including *Pseudomonas aeruginosa*, *Acinetobacter baumannii* and methicillin-resistant *Staphylococcus aureus* (MRSA), using the sequence alignment tool available in the UniProt site, Align (Fig. 5) [25].

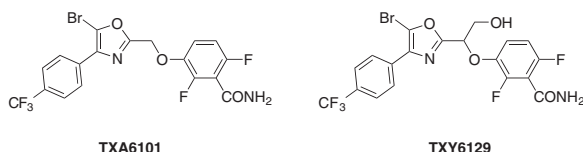


Fig. 4 Structures of two benzamide hits TXA6101 and TXY6129

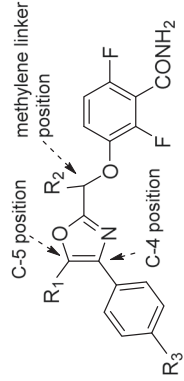
We observed 95–98% homology among members of Enterobacteriaceae, while 50–70% homology of the Enterobacteriaceae family with *S. aureus*, *P. aeruginosa* and *A. baumannii*. Amino acid residues critical for binding our identified hits, such as M226, L261, N263, T309, I/V310, were conserved across all Gram-positive and Gram-negative species. The key difference was observed in residues 193 and 196; while all the Gram-negative species, including *E. coli*, *K. pneumoniae*, *S. sonnei*, and *P. mirabilis* have Alanine instead of Glycine at position 193, Glycine 196 which is critical for TXA707 binding is conserved across all bacteria except *A. baumannii*, where it is replaced by a Serine residue. Since TXA6101 accomplishes FtsZ binding with the G193D mutation, from this sequence alignment data we hypothesized that while TXA707 is not active, TXA6101 should be a potent inhibitor of FtsZ in Enterobacteriaceae family.

Screening of TAXIS library

TAXIS Pharmaceuticals Inc has a library of more than 2,500 FtsZ-targeting molecules that were synthesized and screened for the Gram-positive FtsZ program [22, 23]. Many of the molecules belong to the oxazole benzamide class with varying degrees of FtsZ affinity. Screening of our compound library against Gram-negative pathogens revealed that the TXA6101 chemotype is likely an anti-*K. pneumoniae* drug candidate that achieves MIC values in the $1.0 \mu\text{g mL}^{-1}$ level range. Other compounds in this series (e.g., 3-alkoxy benzamide and oxazole chemotype classes) are also active against wild-type *K. pneumoniae*

<i>K. pneumoniae</i>	174	RGISLLDAFGAANDVLKGA	AVQGIAELITRPGMLNVDFADV	RTVMSEMGYAM	MGSGVASGE	233
<i>E. coli</i>	174	RGISLLDAFGAANDVLKGA	AVQGIAELITRPGMLNVDFADV	RTVMSEMGYAM	MGSGVASGE	233
<i>S. sonnei</i>	174	RGISLLDAFGAANDVLKGA	AVQGIAELITRPGMLNVDFADV	RTVMSEMGYAM	MGSGVANGE	233
<i>P. mirabilis</i>	174	RGISLLDAFGAANDVLKGA	AVQGIAELITRPGMLNVDFADV	RTVMSEMGYAM	MGSGAAKGE	233
<i>P. aeruginosa</i>	175	KDASLLAAFAKADDVLGA	AVRGISDIKRPGMINVDFADV	KTVMSMGMA	MTGCASGP	234
<i>A. baumannii</i>	181	DISMKDAYKKADDVLLN	AVRSIFDLVVRN	GHINLDFADLKTAMSTRGYAM	MGAGLGRGE	239
<i>S. aureus</i> (MRSA)	175	KSTPMMEAFKEADNVL	RGVQGISDLIAVSGEVN	LDFAVKTIMSNQGSAL	MGIGVSSGE	234
<i>K. pneumoniae</i>	234	DRAEEAAEMAISPLLEDID	LSGARGVLVNITAGFDLRLDEFETVGNTIRAF	A-SDNATV		292
<i>E. coli</i>	234	DRAEEAAEMAISPLLEDID	LSGARGVLVNITAGFDLRLDEFETVGNTIRAF	A-SDNATV		292
<i>S. sonnei</i>	234	DRAEEAAEMAISPLLEDID	LSGARGVLVNITAGFDLRLDEFETVGNTIRAF	A-SDNATV		292
<i>P. mirabilis</i>	234	DRAEEAAEMAISPLLEDID	LSGARGVLVNITAGFDLRLDEFETVGNTIRAF	A-SDNATV		292
<i>P. aeruginosa</i>	235	NRAREATEAAIRNP	LLDVLNQGARGILVNITAGPDL	SLGEYS	SDVGNIIQFA-SEHATV	293
<i>A. baumannii</i>	240	DRARQAAEQAIRSP	LLDNVNIINAKGVLINITGGDDITLRETEI	ITDVVNQIVDLDEGEI		299
<i>S. aureus</i> (MRSA)	235	NRAVEAAKKAISPL	LET-SIVGAQGVLMNITGGESLSLFEAQEAADIVQDAA-DEDVNM			292
<i>K. pneumoniae</i>	293	VIGTSLDPDMNDEL	RVTVVATGIGMDKRPEITLV	TNKQVQQPVMDR-YQQHG--MS--PL		347
<i>E. coli</i>	293	VIGTSLDPDMNDEL	RVTVVATGIGMDKRPEITLV	TNKQVQQPVMDR-YQQHG--MA--PL		347
<i>S. sonnei</i>	293	VIGTSLDPDMNDEL	RVTVVATGIGMDKRPEITLV	TNKQVQQPVMDR-YQQHG--MA--PL		347
<i>P. mirabilis</i>	293	VIGTSLDPDMNDEL	RVTVVATGIGMDKRPEITLV	TNKQVQQPVMDR-YQQHG--MA--PL		347
<i>P. aeruginosa</i>	294	KVGTVIDADMRDEL	HVTVATGLGARLEKPKVVDNTVQGSAAQAAAPAQREQQSVNYRD			353
<i>A. baumannii</i>	300	FYGTVPDPARDEL	RVTVVATGLTRNAADAEPKRNTVSHSTQSA-----QSVDE			350
<i>S. aureus</i> (MRSA)	293	IFGTVINPELQDEIVV---	TVATGFDKPTSHGRKSGSTGFGTSVNTS-----SNATS			343

Fig. 5 Alignment of the regions of the amino acid sequences of the FtsZ proteins from *S. aureus*, *K. pneumoniae*, *E. coli*, *P. aeruginosa*, *A. baumannii*, *S. sonnei* and *P. mirabilis*

Table 1 Structure and intrinsic MICs ($\mu\text{g mL}^{-1}$) of representative screened compounds against *K. pneumoniae* (ATCC 10031)


Compound	R ₁	R ₂	R ₃	MIC	Compound	R ₁	R ₂	R ₃	MIC
1 (TXA6101)	Br	H	CF ₃	1	8	Br	CH ₂ OMe	CF ₃	32
2 (TXY6129)	Br	CH ₂ OH	CF ₃	2	9	thiazol-5-yl	H	Cl	64
3	Br	H	Br	2	10	ethynyl	H	Cl	64
4	n-propyl	H	OH	8	11	NH ₂	H	Cl	>256
5	allyl	H	OH	4	12	OMe	H	Cl	>256
6	2-methoxythiazol-5-yl	H	Cl	4	13	CH ₂ NH ₂	H	Cl	>256
7	Cl	CH ₂ OH	Cl	2	14	Br	CH ₂ OH	SO ₂ Me	>256
TXA707	NA ^a	NA ^a	NA ^a	>64					

^aR₁, R₂, and R₃ are not present in TXA707, see Fig. 2

(ATCC 10031). This is in marked contrast to TXA707 and its analogs, which are inactive against *K. pneumoniae*. TXA6101 (compound **1**, Table 1) and TXY6129 (compound **2**, Table 1) are the two most potent FtsZ inhibitors from this series possessing MIC values of $1.0 \mu\text{g mL}^{-1}$ and $2.0 \mu\text{g mL}^{-1}$, respectively. Several structurally-related compounds display potency in the range of $2\text{--}8 \mu\text{g mL}^{-1}$ against wild-type *K. pneumoniae* (ATCC 10031) (Table 1).

This preliminary screen gave us insight into what structural features are required for Gram-negative activity, as well as what features inhibit activity. For example, all active compounds contain a 3-alkoxy-2,6-difluorobenzamide moiety. Compounds di-substituted at the C-4 and C-5 positions of the oxazole ring are the most potent, while the presence of a thiazolo[5,4-b]pyridine ring, common in TXA707-like compounds, was detrimental to activity. It is evident that lipophilic aromatic groups and halogens at the C-4 and C-5 positions of the oxazole ring, respectively, are necessary for Gram-negative activity (Table 1). Polar substitutions at the C-5 position (compounds **11–13**) and on the phenyl ring at the C-4 position (compound **14**) were detrimental to Gram-negative activity. It is also evident that various substitutions on the methylene-linker (R₂) and at the C-5 position of the oxazole ring are moderately tolerated (compounds **8–10**). Compounds **2** and **8**, which have hydroxymethyl substitutions at the pseudo-benzylic position, displayed low MIC values ($2 \mu\text{g mL}^{-1}$) against *K. pneumoniae*. Interestingly, methoxymethyl substitution at the same position reduced potency 16-fold (compound **8** relative to compound **2**). Another interesting finding from our screening was the single digit potency of compounds, **4**, **5**, and **6**: compounds **4** and **5**, contain para-phenol substitutions at the C-4 position, and compound **6**, contains a 2-methoxythiazole-5-yl substitution at the C-5 position.

SAR studies within the oxazole chemotype

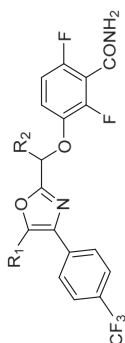
We conducted structure-activity relationship (SAR) studies using TXA6101 (compound **1**, Table 1) and TXY6129 (compound **2**, Table 1).

Substitution of lipophilic groups at the C-5 position (compounds **15** and **16**, Table 2) still maintain potent anti-*K. pneumoniae* activity, albeit less than their halogenated counterparts. Aromatic substitutions at this position seemed to be better tolerated with compounds **15** and **16** yielding MIC values of 8 and $16 \mu\text{g mL}^{-1}$ respectively while cyclopropyl and methyl substitutions at the same position are detrimental (compounds **18** and **19**). This implies that aromatic groups with proper modifications at C-5 of the oxazole ring might produce analogs possessing sub-micromolar potency.

Similarly, the nature of substituents on the methylene-linker (R₂) significantly affected Gram-negative activity

Table 2 Structure and intrinsic MICs ($\mu\text{g mL}^{-1}$) of TXA6101 analogs against *K. pneumoniae* (ATCC 10031)

Compound	R ₁	R ₂	MIC	Compound	R ₁	R ₂	MIC
TXA6101	Br	H	1	TXY6129	Br	CH ₂ OH	2
15	4-Pyr	H	8	20	Br	CH ₂ CH ₂ OH	256
16	4-F-Ph	H	16	21	Br	CH ₂ CH ₂ NH ₂	64
17	Cl	H	4	22	Br	CH ₂ CH ₂ NMe ₂	128
18	cyclopropyl	H	256	23	Br	CH ₂ CH ₂ CH ₂ OH	>256
19	Me	H	256	24	Br	Me	4
TXA707	NA ^a	NA ^a	>64				

^aR₂ and R₃ are not present in TXA707, see Fig. 2

(TXY6129, **20–24**). It is evident from Table 2 that hydroxymethyl substitution at this position is best tolerated, yielding a MIC value of $2.0 \mu\text{g mL}^{-1}$. Changing the number of carbons at the hydroxyalkyl group position greatly affected the MIC values, including hydroxyethyl (compound **20**) and hydroxypropyl (compound **23**) substituents drastically reduced anti-*K. pneumoniae* potency. Another observation that stands out from Table 2 is that changing hydroxy groups to amines somewhat recovered lost potency (compounds **21** and **22**) irrespective of the length of the alkyl chain at this position.

TXA6101, TXY6129 and some analogs are highly potent against efflux compromised *E. coli* strains

We assessed the antibacterial activity of TXA6101, TXY6129 and their analogs versus three different efflux pump deficient strains of *E. coli* (N43, LZ2096, and LZ2310) as well as their isogenic wild-type strain (W4573). Strains N43 and LZ2096 have inactivating mutations in the AcrAB and NorE efflux pumps, respectively, while strain LZ2310 has inactivating mutations in three efflux pumps (AcrAB, NorE and MdfA). CGSC #11430, a TolC knockout mutant strain, was also included. TXA6101, TXY6129 and their analogs are inactive against all bacterial strains (with MIC values $>256 \mu\text{g mL}^{-1}$), except for the single mutant strains N43, CGSC #11430, and the triple mutant strain LZ2310, against which the compounds displayed an MIC of $0.25\text{--}16 \mu\text{g mL}^{-1}$ (Table 3). The over 16-fold enhanced potency of our compounds versus N43 and LZ2310, relative to W4573 and LZ2096, indicates that all the compounds in Table 3 are substrates of the AcrAB-TolC efflux pump in *E. coli*, and not substrates of the NorE efflux pump [26]. Surprisingly, while TXA707 appears also to be a substrate of AcrAB-TolC, treatment with PA β N failed to potentiate it.

To further validate that TXA6101-related types of compounds are indeed substrates of Resistance-Nodulation-Division (RND)-type efflux pumps like AcrAB in *E. coli*, we evaluated the impact of the RND type efflux pump inhibitor PA β N on the activity of TXA6101, TXY6129 and their analogs (Table 3). Use of PA β N lowered the MICs of TXA6101, TXY6129 and some other analogs significantly against wild-type *E. coli* strain (W4573).

Activity of TXA6101 and TXY6129 against other Enterobacteriaceae strains

We explored the potencies of TXA6101 and TXY6129 against additional wild-type strains of *E. coli*, *K. pneumoniae* and other Enterobacteriaceae [27], such as *P. mirabilis* and *S. sonnei*. The results are shown in Table 4. Both the compounds are inactive against all wild-type strains tested, with MIC values greater than $128 \mu\text{g mL}^{-1}$. However, when these

Table 3 Screening of hit compounds against wild-type and efflux-deficient *E. coli* strains

Compound	Intrinsic MIC ($\mu\text{g mL}^{-1}$)					
	W4573 (WT)	N43 (<i>acrAI</i>)	LZ2096 (<i>ΔnorE</i>)	CGSC #11430 (<i>ΔtolC</i>)	LZ2310 (<i>ΔmdfA, ΔnorE, <i>acrAI</i></i>)	W4573 + PA β N(100 $\mu\text{g mL}^{-1}$)
TXA6101	>256	1	>256	≤ 0.25	≤ 0.25	2
TXY6129	>256	2	>256	0.25	0.25	1
4	>256	8	>256	-	-	8
6	>256	8	>256	≤ 0.25	8	4
8	>256	128	>256	-	-	32
15	>256	16	>256	0.25	16	32
16	>256	16	>256	-	-	4
24	>256	2	>256	0.25	0.25	2
TXA707	>64	4	>64	2	>64	>64
Minocycline	2	0.125	2	-	0.25	0.031
Clarithromycin	32	2	-	2	-	≤ 0.25

Table 4 Screening of hit compounds against other Enterobacteriaceae strains in combination with efflux pump inhibitor PA β N (100 $\mu\text{g mL}^{-1}$)

Compound	Intrinsic MIC ($\mu\text{g mL}^{-1}$)							
	<i>E. coli</i> ATCC 25922		<i>K. pneumoniae</i> ATCC 13883		<i>S. sonnei</i> ATCC 29930		<i>P. mirabilis</i> ATCC 29906	
	Alone	+PA β N	Alone	+PA β N	Alone	+PA β N	Alone	+PA β N
TXA6101	>256	≤ 0.25	>256	4	>256	≤ 0.25	>256	>256
TXY6129	>256	0.5	>256	8	128	0.25	>256	128
Clarithromycin	64	≤ 0.25	256	2	64	≤ 0.25	256	256

Table 5 Screening of hit compounds against *P. aeruginosa* and *A. baumannii*

Compound	Intrinsic MIC ($\mu\text{g mL}^{-1}$)			
	<i>P. aeruginosa</i> K767 (WT)	<i>P. aeruginosa</i> K1119 (<i>ΔmexAB-oprM</i>)	<i>A. baumannii</i> BAA-1709	<i>A. baumannii</i> BAA-1709 with PA β N (100 $\mu\text{g mL}^{-1}$)
TXA6101	>256	>256	>256	>256
TXY6129	>256	>256	>256	16
Levofloxacin	1	0.032	-	-
Clarithromycin	-	-	16	≤ 0.25

compounds are combined with EPI PA β N (100 $\mu\text{g mL}^{-1}$) MICs dropped down significantly in all cases with the exception for *P. mirabilis*. Clarithromycin was used as a positive control since it is known to be potentiated by PA β N. It is apparent that these classes of compounds are good substrates of RND efflux pumps in all Enterobacteriaceae pathogens.

Activity of TXA6101 and TXY6129 against *P. aeruginosa* and *A. baumannii*

We also investigated the potencies of our two hit compounds against other important Gram-negative pathogens,

such as *P. aeruginosa* and *A. baumannii* (Table 5). Both hit compounds were inactive against wild-type *P. aeruginosa*. Deleting one of the multiple RND efflux pumps in *P. aeruginosa*, MexAB-OprM, resulted in enhanced sensitivity to levofloxacin but did not lead to TXA6101 or TXY6129 activity. A clinical isolate of *A. baumannii*, BAA-1709, is also insensitive to TXA6101 and TXY6129. Use of PA β N did not enhance the potencies of these two compounds to any significant level while the activity of clarithromycin (known substrates of RND-type efflux pumps) was predictably enhanced by PA β N. Thus, as evident in Table 5, our compounds have no impact on either wild-type or efflux-deficient *P. aeruginosa* and *A. baumannii*. Since

Fig. 6 Differential interference contrast (DIC) micrographs of *E. coli* N43 cells treated for 3 h with either DMSO vehicle (left), 4 $\mu\text{g mL}^{-1}$ (4XMIC) TXA6101 (center), or 4 $\mu\text{g mL}^{-1}$ (4XMIC) TXY6129 (right). Scale bar reflects 5 μm

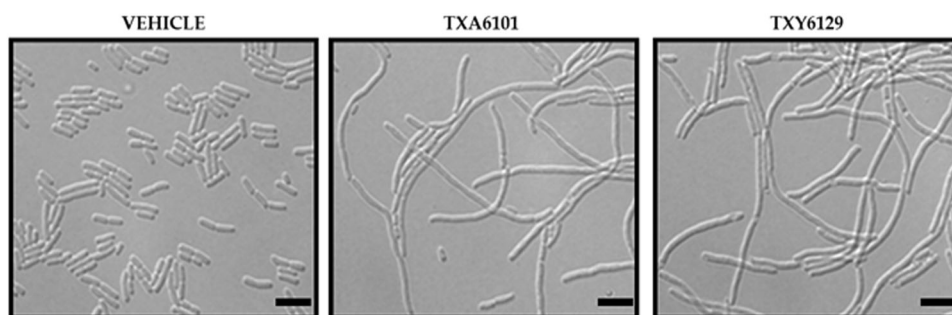


Fig. 7 Differential interference contrast (DIC) micrographs of *K. pneumoniae* ATCC 10031 cells treated for 3 h with either DMSO vehicle (left), 4 $\mu\text{g mL}^{-1}$ (4XMIC) TXA6101 (center), or 8 $\mu\text{g mL}^{-1}$ (4XMIC) TXY6129 (right). Scale bar reflects 5 μm

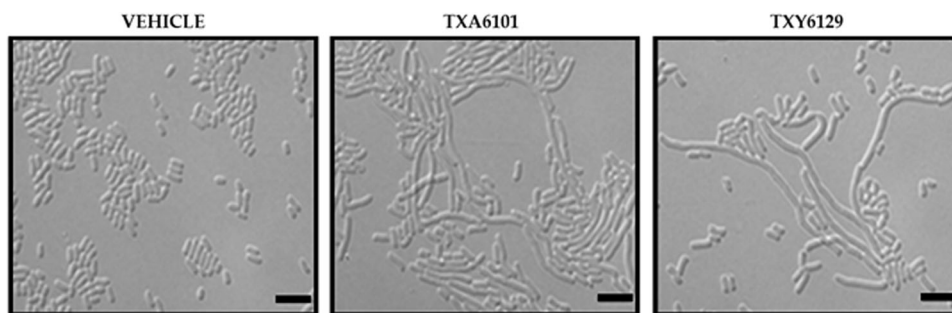
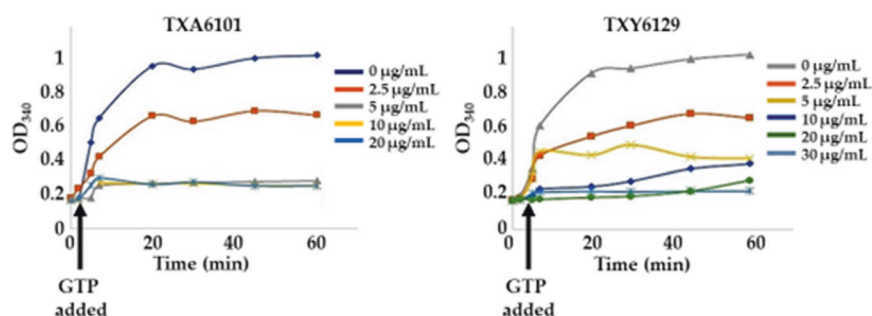


Fig. 8 Concentration dependence of the impact of TXA6101 and TXY6129 on the polymerization of *E. coli* FtsZ, as determined by monitoring time-dependent changes in absorbance at 340 nm (OD_{340}) at 25 °C



TXA6101 and TXY6129 showed no activity against *P. aeruginosa* and *A. baumannii* in the presence or absence of efflux pumps or with an EPI, it may be concluded that the inactivity of these agents is due to an inability of the compound to target the FtsZ proteins in these bacteria rather than the actions of RND-type efflux pumps in these bacteria. Alternative reasons for the lack of activity in *P. aeruginosa* could be that an RND efflux pump other than MexAB-OprM is responsible for the efflux of our hit compounds, or, that *P. aeruginosa* is impermeable to TXA6101 and TXY6129.

TXA6101 and TXY6129 induce morphological changes in *K. pneumoniae* and *E. coli*

TXA6101 and TXY6129 induce changes in the morphology of *E. coli* and *K. pneumoniae* consistent with inhibition of cell division. To probe whether TXA6101 and TXY6129 can target the FtsZ protein in *K. pneumoniae* and *E. coli*, we measured the effect of the compounds on the morphology of

these bacteria, utilizing phase-contrast microscopy. *K. pneumoniae* and *E. coli* bacteria treated with TXA6101 and TXY6129 appear as long filaments 5- to 10-fold longer than vehicle-treated bacteria, which are short 1-2 μm rods (Figs. 6 and 7). This morphological change in both *K. pneumoniae* and *E. coli* induced by TXA6101 and TXY6129 is a characteristic feature of FtsZ-targeting inhibitors. This result is consistent with the hypothesis that, in addition to the ability of TXA6101 to target *S. aureus* FtsZ, the compound also targets *K. pneumoniae* and *E. coli* FtsZ.

TXA6101 and TXY6129 inhibit the polymerization of *E. coli* FtsZ in a concentration-dependent manner

In order to examine if TXA6101 and TXY6129 impact the polymerization activity of *E. coli* FtsZ protein, we utilized a microtiter plate-based spectrophotometric assay in which FtsZ polymerization and bundling is detected in solution by a time dependent increase in solution absorbance at 340 nm (OD_{340}) [27]. Figure 8 shows the time-dependent OD_{340}

Table 6 Antimicrobial property of TXA6101 and TXY6129

Compound	<i>K. pneumoniae</i> ATCC 10031				<i>E. coli</i> N43			
	MIC ($\mu\text{g mL}^{-1}$)	MBC ($\mu\text{g mL}^{-1}$)	MBC/MIC	Presumptive property	MIC ($\mu\text{g mL}^{-1}$)	MBC ($\mu\text{g mL}^{-1}$)	MBC/MIC	Presumptive property
TXA6101	1	4	4	Bactericidal	1	2	2	Bactericidal
TXY6129	2	8	4	Bactericidal	2	8	4	Bactericidal
Ceftazidime	0.125	0.25	2	Bactericidal	0.25	0.25	1	Bactericidal
Clarithromycin	4	32	8	Bacteriostatic	8	32	4	Bactericidal

Table 7 FIC index values of TXA6101 with five β -lactam antibiotics against *K. pneumoniae* ATCC10031

Ceftazidime & TXA6101		Piperacillin & TXA6101		Cefdinir & TXA6101		Aztreonam & TXA6101		Imipenem & TXA6101		Clarithromycin & TXA6101	
ΣFIC	Activity	ΣFIC	Activity	ΣFIC	Activity	ΣFIC	Activity	ΣFIC	Activity	ΣFIC	Activity
0.49	Synergy	0.38	Synergy	0.38	Synergy	0.38	Synergy	0.31	Synergy	2	Indifference

ΣFIC : ≤ 0.5 synergy; 0.5–4 indifference; >4 additive

profiles of *E. coli* FtsZ (Cytoskeleton, Inc), in the presence of both TXA6101 and TXY6129, at concentrations ranging from 0 to 30 $\mu\text{g mL}^{-1}$. Note that the presence of TXA6101 and TXY6129 decreases the extent of *E. coli* FtsZ polymerization/bundling, with the magnitude of these inhibitory effects increasing with increasing compound concentration. Thus, in presence of TXA6101 and TXY6129 polymerization and/or bundling of *E. coli* FtsZ is inhibited.

TXA6101 and TXY6129 are bactericidal

We used microdilution methods to determine minimum bactericidal concentration (MBC) and calculated the ratio of MBC over MIC according to the CLSI standardized protocol. Both hit compounds are considered to be bactericidal according to the CLSI standard (MBC/MIC is ≤ 4) [28] This result is consistent with our FtsZ targeting drug candidate, TXA707 (Table 6).

TXA6101 is synergistic with beta-lactam antibiotics

Given the involvement of FtsZ and the penicillin-binding proteins in a common pathway [29] leading to septum formation and cell division, to explore the potential for synergy with TXA6101, we conducted checkerboard antibacterial assays in which growth inhibition is monitored at differing concentration ratios of two complementary test agents. The checkerboard assays enabled us to determine fractional inhibitory concentrations (FICs) at each drug combination that inhibits growth by $\geq 90\%$. Synergy is indicated by an $\text{FIC}_{\text{index}} \leq 0.5$. Consistent with our hypothesis, 5 β -lactam antibiotics act synergistically with our FtsZ inhibitor TXA6101 against *K. pneumoniae* ATCC 10031.

As shown in Table 7, all five combinations had synergistic effect against the bacterium with FIC indexes ranging from 0.31 to 0.49. Clarithromycin as a negative control does not have synergistic effect with an FIC index 2.

Materials and methods

Materials

Cation adjusted Mueller-Hinton (CAMH) broth, trypticase soy agar (TSA) were obtained from Becton, Dickinson and Company (MD, USA). Phe-Arg β -naphthylamide (PA β N) dihydrochloride was purchased from Sigma-Aldrich (MO, USA). Levofloxacin, clarithromycin, ceftazidime, piperacillin, cefdinir, aztreonam, imipenem and minocycline were purchased from TOKU-E (WA, USA). *E. coli* FtsZ protein was purchased from Cytoskeleton, Inc (CO, USA).

Bacterial strains

E. coli W4573, N43 (*acrA1*), LZ2096 (ΔnorE), and LZ2310 (*acrA1* ΔmdfA ΔnorE) were gifts from Dr. Lynn Zechiedrich (Baylor College of Medicine, Houston, TX). *E. coli* CGSC #11430 (*ΔtolC*) was obtained from the Coli Genetic Stock Center (YALE University, New Haven, CT). *E. coli* ATCC 25922, *K. pneumoniae* ATCC 10031, *K. pneumoniae* ATCC 13883, *S. sonnei* ATCC 29930, *A. baumannii* BAA-1709 and *P. mirabilis* ATCC 29906 were obtained from the American Type Culture Collection (Manassas, VA). *P. aeruginosa* K767 and K1119 ($\Delta\text{mexAB-oprM}$) was obtained from Professor Keith Poole (Queen's University, Kingston, ON, Canada).

Compound synthesis

The synthesis and characterization of reported compounds have been described in Patent US9511073.

DNA sequence analysis

Multiple protein sequence alignments were performed in the UniProt website (with the Clustal Omega algorithm) [25].

MIC assays

MIC assays were conducted in accordance with Clinical and Laboratory Standards Institute (CLSI) guidelines for broth microdilution [28]. Briefly, log-phase bacteria were added to 96-well microtiter plates (at 5×10^5 CFU ml⁻¹) containing 2-fold serial dilutions of compound or comparator drug in CAMH broth, with each compound concentration being present in duplicate. The final volume in each well was 0.1 mL, and the microtiter plates were incubated aerobically for 24 h at 37 °C. Bacterial growth was then monitored by measuring the optical density at 600 nm using a VersaMax plate reader (Molecular Devices, Inc.), with the MIC being defined as the lowest compound concentration at which growth was $\geq 90\%$ inhibited.

MBC assays

MBC assays were conducted in accordance with CLSI guidelines [28]. Broth microdilution assays were conducted as described in the preceding section. After the 24-h incubation period, aliquots from the microtiter wells were plated onto TSA. The colonies that grew after 24 h of incubation were counted, with MBC being defined as the lowest compound concentration resulting in a ≥ 3 -log reduction in the number of CFU.

EPI assays

MIC for the test compounds were determined as described above in the absence and presence of sub-inhibitory concentrations of commercial PA β N. PA β N was used at 100 μ g mL⁻¹.

Differential interference contrast (DIC) microscopy

DIC micrographs of *E. coli* N43 and *K. pneumoniae* ATCC 10031 treated with DMSO (vehicle), TXA6101 or TXA6129 were performed as described previously [30].

FtsZ polymerization assay

Polymerization of *E. coli* FtsZ was monitored using a microtiter plate-based spectrophotometric assay in which changes in FtsZ polymerization are reflected by corresponding changes in absorbance at 340 nm (A340). TXA6101 or TXY6129 (at concentrations ranging from 0 to 30 μ g mL⁻¹) were combined with 5 μ M FtsZ in 100 μ L of reaction solution. Reaction solutions contained 50 mM Tris-HCl (pH 7.4), 50 mM KCl, and 10 mM magnesium acetate. Reactions were assembled in half-volume, flat-bottom, 96-well microtiter plates and initiated by the addition of 4 mM GTP. Polymerization was continuously monitored at 25 °C by measuring A340 in a VersaMax plate reader over a period of 60 min.

Checkerboard assay

The checkerboard titration method was used to evaluate synergy between TXA6101 and ceftazidime, piperacillin, cefdinir, aztreonam, imipenem or clarithromycin against *K. pneumoniae* ATCC 10031. In this assay (performed with 96-well microtiter plates), TXA6101 was serially diluted twofold in CAMH broth along the rows of the microtiter plate, while the other antibiotics were diluted along the columns. The final volume in each well was 0.1 mL. After the compounds were added, each well was inoculated with 5×10^5 CFU of log-phase bacteria. The microtiter plates were incubated aerobically for 16–24 h at 37 °C, at which point bacterial growth was visualized. Fractional inhibitory concentrations (FICs) of the agents in each well that did not exhibit visible growth compared to agent-free control wells were calculated with the following two relationships: (i) $FIC_{TXA6101} = MIC \text{ of TXA6101 in combination with antibiotic} / MIC \text{ of TXA6101 alone}$; (ii) $FIC_{\text{antibiotic}} = MIC \text{ of antibiotic in combination with TXA6101} / MIC \text{ of antibiotic alone}$. These FICs allow the determination of the FIC index (FICI) with the following relationship: $FICI = FIC_{TXA6101} + FIC_{\text{antibiotic}}$. An FICI of ≤ 0.5 indicates synergy between the two agents, an FICI between 0.5 and 4.0 indicates indifference, and an FICI > 4 indicates additivity.

Conclusions

We have shown that oxazole benzamides are good substrates of RND efflux pumps in the Enterobacteriaceae family of Gram-negative bacteria. Either removing RND pumps or combining our compounds with efflux pump inhibitors (EPIs) conferred high potency against Enterobacteriaceae pathogens. We proved that these inhibitors do target FtsZ protein. In order for them to become inhibitors worthy of development against Enterobacteriaceae, their efflux liability needs to be

eliminated. These issues can be overcome by designing new molecules within the same chemotype to evade efflux pumps thus rendering them with higher potency. Alternatively, developing combination therapies that pair FtsZ inhibitors with safe EPIs could provide new treatment options against Gram-negative infections. Efforts to achieve both strategies are currently underway at TAXIS Pharmaceuticals Inc and will be reported in due course.

Patents

The synthesis, characterization and bioactivity of some reported compounds have been described in Patent US9511073.

Acknowledgements We are indebted to Prof. Edmond J. LaVoie for providing scientific inputs. We are also indebted to Prof. Daniel Pilch and Dr. Edgar Ferrer-González for providing us with the differential interference contrast (DIC) micrographs and with the *E. coli* W4573, N43 (acrA1), LZ2096 (Δ norE), and LZ2310 (acrA1 Δ mdfA Δ norE) strains.

Author contributions Conceptualization, AP; methodology, AP and JR; investigation, JR; YS; AB; YC; PD; YZ, and YY; writing—original draft preparation, AP; writing—review and editing, YY; JR; supervision, AP; project administration, AP; JR; and YS; All authors have read and agreed to the published version of the manuscript.

Compliance with ethical standards

Conflict of interest AP, JR, PD, and YZ are employees of TAXIS Pharmaceuticals, Inc. and, therefore, have a financial interest in the company.

Publisher's note Springer Nature remains neutral with regard to jurisdictional claims in published maps and institutional affiliations.

References

1. WHO Global antimicrobial resistance surveillance system (GLASS) report: early implementation 2016–2017. Geneva: World Health Organization; 2017.
2. O'Neill J. Tackling drug-resistant infections globally: final report and recommendations: Government of the United Kingdom; 2016.
3. Laxminarayan R, Duse A, Wattal C, Zaidi AK, Wertheim HF, Sumpradit N, et al. Antibiotic resistance—the need for global solutions. *Lancet Infect Dis*. 2013;13:1057–98.
4. Luepke KH, Suda KJ, Boucher H, Russo RL, Bonney MW, Hunt TD, et al. Past, present, and future of antibacterial economics: increasing bacterial resistance, limited antibiotic pipeline, and societal implications. *Pharmacotherapy*. 2017;37:71–84.
5. Perez F, Van Duin D. Carbapenem-resistant Enterobacteriaceae: a menace to our most vulnerable patients. *Cleve Clin J Med*. 2013;80:225–33.
6. Tzouveleakis LS, Markogiannakis A, Psychogiou M, Tassios PT, Daikos GL. Carbapenemases in *Klebsiella pneumoniae* and other Enterobacteriaceae: an evolving crisis of global dimensions. *Clin Microbiol Rev*. 2012;25:682–707.
7. Adams DW, Errington J. Bacterial cell division: assembly, maintenance and disassembly of the Z ring. *Nat Rev Microbiol*. 2009;7:642–53.
8. Bi EF, Lutkenhaus J. FtsZ ring structure associated with division in *Escherichia coli*. *Nature*. 1991;354:161–4.
9. Erickson HP, Anderson DE, Osawa M. FtsZ in bacterial cytokinesis: cytoskeleton and force generator all in one. *Microbiol Mol Biol Rev*. 2010;74:504–28.
10. Awasthi D, Kumar K, Ojima I. Therapeutic potential of FtsZ inhibition: a patent perspective. *Expert Opin Ther Pat*. 2011;21:657–79.
11. Hurley KA, Santos TM, Nepomuceno GM, Huynh V, Shaw JT, Weibel DB. Targeting the bacterial division protein FtsZ. *J Med Chem*. 2016;59:6975–98.
12. Carro L. Recent progress in the development of small-molecule ftsz inhibitors as chemical tools for the development of novel antibiotics. *Antibiotics*. 2019; 8.
13. Kusuma KD, Payne M, Ung AT, Bottomley AL, Harry EJ. FtsZ as an antibacterial target: status and guidelines for progressing this avenue. *ACS Infect Dis*. 2019;5:1279–94.
14. Schaffner-Barbero C, Martin-Fontecha M, Chacon P, Andreu JM. Targeting the assembly of bacterial cell division protein FtsZ with small molecules. *ACS Chem Biol*. 2012;7:269–77.
15. Artola M, Ruiz-Avila LB, Vergonos A, Huecas S, Araujo-Bazan L, Martin-Fontecha M, et al. Effective GTP-replacing FtsZ inhibitors and antibacterial mechanism of action. *ACS Chem Biol*. 2015;10:834–43.
16. Singh D, Bhattacharya A, Rai A, Dhaked HP, Awasthi D, Ojima I, et al. SB-RA-2001 inhibits bacterial proliferation by targeting FtsZ assembly. *Biochemistry*. 2014;53:2979–92.
17. Haydon DJ, Stokes NR, Ure R, Galbraith G, Bennett JM, Brown DR, et al. An inhibitor of FtsZ with potent and selective anti-staphylococcal activity. *Science*. 2008;321:1673–5.
18. Kaul M, Mark L, Zhang Y, Parhi AK, LaVoie EJ, Pilch DS. Pharmacokinetics and in vivo antistaphylococcal efficacy of TXY541, a 1-methylpiperidine-4-carboxamide prodrug of PC190723. *Biochem Pharm*. 2013;86:1699–707.
19. Kaul M, Mark L, Zhang Y, Parhi AK, LaVoie EJ, Pilch DS. An FtsZ-targeting prodrug with oral antistaphylococcal efficacy in vivo. *Antimicrob Agents Chemother*. 2013;57:5860–9.
20. Kaul M, Mark L, Zhang Y, Parhi AK, Lyu YL, Pawlak J, et al. TXA709, an FtsZ-targeting benzamide prodrug with improved pharmacokinetics and enhanced in vivo efficacy against methicillin-resistant *Staphylococcus aureus*. *Antimicrob Agents Chemother*. 2015;59:4845–55.
21. Lepak AJ, Parhi A, Madison M, Marchillo K, VanHecker J, Andes DR. In vivo pharmacodynamic evaluation of an FtsZ inhibitor, TXA-709, and its active metabolite, TXA-707, in a murine neutropenic thigh infection model. *Antimicrob Agents Chemother*. 2015;59:6568–74.
22. Stokes NR, Baker N, Bennett JM, Berry J, Collins I, Czaplowski LG, et al. An improved small-molecule inhibitor of FtsZ with superior in vitro potency, drug-like properties, and in vivo efficacy. *Antimicrob Agents Chemother*. 2013;57:317–25.
23. Stokes NR, Baker N, Bennett JM, Chauhan PK, Collins I, Davies DT, et al. Design, synthesis and structure-activity relationships of substituted oxazole-benzamide antibacterial inhibitors of FtsZ. *Bioorg Med Chem Lett*. 2014;24:353–9.
24. Fujita J, Maeda Y, Mizohata E, Inoue T, Kaul M, Parhi AK, et al. Structural flexibility of an inhibitor overcomes drug resistance mutations in *Staphylococcus aureus* FtsZ. *ACS Chem Biol*. 2017;12:1947–55.
25. UniProt C. UniProt: a worldwide hub of protein knowledge. *Nucleic Acids Res*. 2019;47:D506–D15.
26. Kaul M, Zhang Y, Parhi AK, Lavoie EJ, Pilch DS. Inhibition of RND-type efflux pumps confers the FtsZ-directed prodrug

- TXY436 with activity against Gram-negative bacteria. *Biochem Pharm.* 2014;89:321–8.
27. Kaul M, Zhang Y, Parhi AK, Lavoie EJ, Tuske S, Arnold E, et al. Enterococcal and streptococcal resistance to PC190723 and related compounds: molecular insights from a FtsZ mutational analysis. *Biochimie* 2013;95:1880–7.
 28. CLSI Methods for dilution antimicrobial susceptibility tests for bacteria that grow aerobically; approved standard—Tenth Edition. Wayne, PA 2015.
 29. Kaul M, Mark L, Parhi AK, LaVoie EJ, Pilch DS. Combining the FtsZ-targeting prodrug TXA709 and the Cephalosporin Cefdinir Confers Synergy and Reduces the Frequency of Resistance in Methicillin-resistant *Staphylococcus aureus*. *Antimicrob Agents Chemother.* 2016;60:4290–6.
 30. Ferrer-Gonzalez E, Fujita J, Yoshizawa T, Nelson JM, Pilch AJ, Hillman E, et al. Structure-guided design of a fluorescent probe for the visualization of FtsZ in clinically important gram-positive and gram-negative bacterial pathogens. *Sci Rep.* 2019;9:20092.